VI International Conference on Adaptive Modeling and Simulation
ADMOS 2013
J. P. Moitinho de Almeida, P. Díez, C. Tiago and N. Parés (Eds)

CONSTRUCTION OF DYNAMICALLY ADAPTING COMPUTATIONAL GRIDS IN SYSTEMS OF DIFFERENTIAL EQUATIONS DESCRIBING THE NON-EQUILIBRIUM PROCESSES

ALEXANDER V. MAZHUKIN*, OLGA N. KOROLEVA†

* Keldysh Institute of Applied Mathematics
125047 Miusskaya sq. 4 Moscow, Russia
e-mail: vim@modhef.ru

† Moscow University for the Humanities
111395 Yunosti st. 5 Moscow, Russia
email: koroleva.on@mail.ru

Key words: Modeling, Adaptive grid, Dynamic adaptation, Systems of differential equations, Laser irradiation.

Abstract. The processes occurring in solid targets (metals, semiconductors) initiated by pulsed flows of condensed energy is described by two-temperature model (TTM). The simplest TTM model for metals consists of two, and for semiconductors of three non-linear parabolic equations. Ultrafast impact (pico-femtosecond pulse duration) predetermines the appearance of large solution gradients that require in numerical solution application of computational grids with dynamic adaptation. Transition to an arbitrary non-stationary system of coordinates, the velocity of which is unknown and depends on the desired solution is the basis of the construction of a dynamically adaptive grids. Velocity of the system of coordinates for the numerical discretization is used as a function that control the motion of grid nodes . Agreed change of movement of grid nodes with the solution is achieved by constructing of transformation function derived from the principle of quasi-stationarity.

Simulation of some specific regimes of pulsed heating and melting of semiconductor silicon (Si), using a numerical grid with the controlled distribution of nodes was carried out.

1 INTRODUCTION

Pulsed laser radiation is a widely used tool for precision machining of materials, including semiconductors. Among semiconductor materials, silicon was most widespread in the instrument-making and is one of the most promising materials for thin-film nanotechnology.

To optimize existing and develop new technologies of laser surface treatment of semiconductors it is necessary to perform a detailed study of the dynamics of processes occurring in the irradiation zone and leading to surface modification, including an analysis of the processes of heating, melting and evaporation.

In this paper, we use the methods of mathematical modeling to investigate the action of laser pulse (picosecond) with a wave length of $\lambda_L=0.53\mu m$ and the photon energy exceeding the band gap of silicon target $\hbar\omega>E_g$. The main feature of these regimes of laser action is

highly non-equilibrium of heating and melting processes, which results in a large difference between the carriers temperature and the lattice temperature. The numerical solution of system of partial differential equations of parabolic type was carried out by means of the dynamic adaptation method. The use of arbitrary nonstationary system of coordinates allows to construct grids with a constant number of nodes in regions with moving boundaries and allows to concentrate grid nodes in regions of large gradients of solutions.

Laser radiation with intensity $G(t)$, Gaussian distribution and wavelength λ_L extending from left to right (Fig. 1) falls on silicon target surface, where the part of the radiation is reflected and some is absorbed. The released energy of laser pulse causes heating, melting (moving boundary Γ_{sl} - melting front) and evaporation (moving boundary Γ_{lv} - evaporation front).

2 MODEL

The mathematical model consists of transport equations of the laser radiation, which takes into account the temperature dependence of the reflectivity of the surface, the carrier balance equation that takes into account generation (photo-ionization) and recombination of charged particles (Auger recombination, and photo-recombination), the balance equations of energy carriers and the lattice, taking into account the absorption of laser energy, the exchange of energy between the electron and phonon subsystems, heat and mass transfer [1-2].

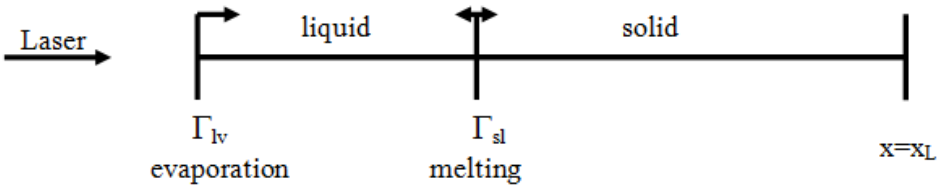

Figure 1. Scheme of laser irradiation.

The basis of first-order phase transitions is the mechanism of heterogeneous melting and evaporation. The process of melting - crystallization is described in approximation of classical variant of Stefan problem and the process of evaporation is described in approximation of Knudsen layer (single-phase version of Stefan problem).

Semiconductor has the properties of metal after melting temperature is reached. And therefore it is necessary to write equations for the solid and liquid regions.

Equations for solid region:

$$\frac{\partial N}{\partial t} = -\frac{\partial J}{\partial x} + I_{en} - R_{en}, \tag{1}$$

$$\frac{\partial \varepsilon_e}{\partial t} = -\frac{\partial W_e}{\partial x} - \frac{\partial G}{\partial x} - g(T_e)_{lat}(T_e - T_{lat}), \tag{2}$$

$$\frac{\partial \varepsilon_{lat}}{\partial t} = -\frac{\partial W_{lat}}{\partial x} + g(T_e)_{lat}(T_e - T_{lat}), \tag{3}$$

$$\frac{\partial G}{\partial x} = -(\alpha + \beta_1)G - \beta_2 G^2, \tag{4}$$

$$\Gamma_{sl} < x < x_L$$

Equation (1) is equation for a concentration. Equations (2), (3) are energy equations for electron component and lattice. Equation (4) is equation of laser energy transfer.

Equations for liquid region:

$$\frac{\partial \varepsilon_e}{\partial t} = \frac{\partial}{\partial x}\left(\lambda_e(T_e, T_l)\frac{\partial T_e}{\partial x}\right) - g(T_e)(T_e - T_l) - \frac{\partial G}{\partial x} \tag{5}$$

$$\frac{\partial \varepsilon_l}{\partial t} = \frac{\partial}{\partial x}\left(\lambda_l(T_l)\frac{\partial T_l}{\partial x}\right) + g(T_e)(T_e - T_l) \tag{6}$$

$$\frac{\partial G}{\partial x} = -\alpha G, \qquad G(t) = G_0 \exp\left(-\left(\frac{t}{\tau}\right)^2\right) \tag{7}$$

$$\Gamma_{l\upsilon} < x < \Gamma_{sl}$$

Where N – carrier concentration, J – particle current density, ε_e и ε_{lat} – internal energy of electron gas and lattice, W_e и W_{lat} – heat flow of electron gas and lattice, x_L – right end of the sample, λ_e и λ_l – heat conductivity coefficient of electron gas and liquid metal, $I_{en} = \frac{\beta_1 G}{\hbar\omega} + \frac{\beta_2 G^2}{2\hbar\omega} + k_i(T_e)N$ and $R_{en}=\gamma N^3$ – electron-hole pairs generation and recombination velocities, γ - Auger recombination coefficient and ω - laser irradiation frequency, α – free-carrier absorption coefficient, β_1 and β_2 - coefficients of one and two photon absorption, k_i - collision ionization coefficient, $g(T_e)$, $g(T_e)_{lat}$ – electron-lattice energy exchange factor for metal and semiconductor, $g(T_e)_{lat}=C_e/\tau_E$, τ_E - energy relaxation time, C_e – heat capacity. $g(T_e)$ and other thermophysical properties of metals reported in [4].

Equations (5), (6) are energy equations for electron component and lattice one. Equation (7) is equation of laser energy transfer.

Boundary conditions:

$x = x_L$: $J = 0,\ W_e = W_{lat} = 0$

$x = \Gamma_{sl}(t)$: for electron component: $(W_e)_s = (W_e)_l,\ (T_e)_s = (T_e)_l,$

for lattice: $T_s = T_l = T_m,\ \left(\lambda_{lat}\frac{\partial T_{lat}}{\partial x}\right)_s - \left(\lambda_{lat}\frac{\partial T_{lat}}{\partial x}\right)_l = \rho_s L_m \upsilon_{sl},$

$x = \Gamma_{lv}(t)$: for electron component: $J = 0,\ W_e = 0,\ G_l(t) = AG(t)$

for lattice:

$$\lambda\frac{\partial T_l}{\partial x}=\rho_l L_\upsilon \upsilon_{l\upsilon}, \qquad \rho_l\upsilon_{l\upsilon}=\rho_\upsilon\left(\upsilon_{l\upsilon}-u\right)$$

$$P_l+\rho_l\upsilon_{l\upsilon}^2=P_\upsilon+\rho_\upsilon\left(\upsilon_{l\upsilon}-u\right)^2$$

$$T_\upsilon=0.633T_l, \quad \rho_\upsilon=0.326\rho_{sat}, \quad u=\left(\gamma RT_\upsilon\right)^{1/2}$$

$$\rho_{sat}=\frac{P_{sat}}{RT_l}, \quad P_{sat}=p_b\exp\left[\frac{L_v}{RT_b}\left(1-\frac{T_b}{T_l}\right)\right]$$

Indexes *lat, l, v, s, sat, b* mean values affiliation to semiconductor lattice, metal liquid phase, vapor, solid phase, saturated vapor and boiling under normal conditions.

3 METHOD

The method of dynamic adaptation is based on a transition to an arbitrary non-stationary coordinate system. The usage of an arbitrary non-stationary coordinate system allows to formulate the problem of the grid generation and adaptation at the differential level, i.e. in the resulting mathematical model, one part of the differential equations describes the physical processes and the other part – the behavior of the nodes of the grid [5]. The transition to an arbitrary non-stationary coordinate system is performed using an automated coordinate transformation via the sought solution.

According to the papers [5] – [7], we will perform a transition from the physical space $\Omega_{\mathrm{x,t}}$ with Euler variables (x,t) to some computational space with an arbitrary non-stationary coordinate system $\Omega_{q,\tau}$ with variables (q,τ). This transformation can be performed using a substitution of variables of a common form $x=f(q,\tau), \quad t=\tau$, with a single-valued non-degenerate reverse transformation $q=\varphi(x,t), \quad \tau=\mathrm{t}$.

During the transition from one coordinate system to another, the partial derivatives of the dependent variables are connected via the following expressions:

$$\frac{\partial}{\partial t}=\frac{\partial}{\partial\tau}+\frac{Q}{\psi}\frac{\partial}{\partial q}; \quad \frac{\partial}{\partial x}=\frac{1}{\psi}\frac{\partial}{\partial q}; \quad \frac{\partial^2}{\partial x^2}=\frac{1}{\psi}\frac{\partial}{\partial q}\frac{1}{\psi}\frac{\partial}{\partial q} \tag{8}$$

where $\psi=\partial x/\partial q$ - is the Jacobian of the reverse transformation.

Using a replacement of variables of the common form and expressions (8), we can write the differential model (1) –(4) and (5) – (7) in the variables (q,τ):

$$\frac{\partial(\psi N)}{\partial\tau}=-\frac{\partial(Q_s N)}{\partial q}-\frac{\partial J}{\partial q}-\psi\left(R_{en}-I_{en}\right) \tag{9}$$

$$\frac{\partial(\psi\varepsilon_{\ell at})}{\partial\tau}=-\frac{\partial(Q_s\varepsilon_{\ell at})}{\partial q}+\psi q_e(T_e)(T_e-T_{\ell at})-\frac{\partial W_{\ell at}}{\partial q} \tag{10}$$

$$\frac{\partial(\psi\varepsilon_e)}{\partial\tau}=-\frac{\partial(Q_s\varepsilon_e)}{\partial q}-\frac{\partial G}{\partial q}-\psi q_e(T_e)(T_e-T_{eat})-\frac{\partial W_e}{\partial q} \tag{11}$$

$$\frac{\partial G}{\partial q}=-\psi(\alpha+\beta_1)G-\psi\beta_2G^2 \tag{12}$$

$$\frac{\partial\psi}{\partial\tau}=-\frac{\partial Q_s}{\partial q} \tag{13}$$

$$\Gamma_{sl} < x < x_L, \qquad \tau > 0$$

$$\frac{\partial(\psi \varepsilon_e)}{\partial \tau} = -\frac{\partial(Q_\ell \varepsilon_e)}{\partial q} - \frac{\partial W_e}{\partial q} - \frac{\partial G}{\partial q} - \psi g(T_e)(T_e - T_\ell) \tag{14}$$

$$\frac{\partial(\psi \varepsilon_\ell)}{\partial \tau} = -\frac{\partial(Q_\ell \varepsilon_\ell)}{\partial q} - \frac{\partial W_\ell}{\partial q} + \psi g(T_e)(T_e - T_\ell) \tag{15}$$

$$\frac{\partial G}{\partial q} = -\psi \alpha G \tag{16}$$

$$\frac{\partial \psi}{\partial \tau} = -\frac{\partial Q_\ell}{\partial q} \tag{17}$$

$$\Gamma_{\ell\upsilon} < x < \Gamma_{s\ell}, \qquad \tau > 0$$

where (13), (17) – are the equations of the reverse transformation with the transformation functions Q_s, Q_ℓ. The functions Q_s, Q_ℓ characterize the speed of the non-stationary coordinate system in the solid and liquid phases accordingly and are not predefined and should be determined.

Thus, during the transition to an arbitrary non-stationary coordinate system, the initial differential models are transformed to the extended differential systems with additional equations (13) and (17). Their type, properties and form of the boundary conditions depend on the particular form of the functions Q [7]. At this stage of discussion, the functions Q_s, Q_ℓ are not defined yet. After their determination, the equations (13) and (17) are used for construction of the grids that adapt to the gradients of solution and to the moving domain boundaries. Their differential analogues describe the dynamics of the grid nodes and the functions Q_s, Q_ℓ perform the controlled motion of the grid nodes in an agreement with the dynamics of the sought solution. The agreement is achieved by introduction of a functional dependency of the function Q on the sought solution. But since the solution is not known beforehand, a problem arises with the determination of the optimum transformation function Q that will provide a complete matching of the adaptation mechanism with the solution. If there are no complete matching, fitting coefficients are inserted into the controlling function. By the adjustment of the fitting coefficients, it is possible to make the degree of the mismatching lower. At the same time, the fact of the presence of the fitting coefficients in an adaptation method is an evidence of its imperfection.

Such matching can be obtained using the quasi-stationary principle [1], [8], which states that it is necessary to switch to a such coordinate system, where the time derivatives will be small or satisfy the relation: $\partial N/\partial\tau = \partial\varepsilon_e/\partial\tau = \partial\varepsilon_{\ell at}/\partial\tau = \partial\varepsilon_\ell/\partial\tau = 0$. Then the transformation functions will take the form:

$$Q_s = -\frac{\dfrac{\partial W_e}{\partial q} + \dfrac{\partial W_{\ell at}}{\partial q} + \dfrac{\partial G}{\partial q} + \dfrac{\partial J}{\partial q} + \psi\left(R_{en} - I_{en}\right)}{\left|\dfrac{\partial N}{\partial q}\right| + \left|\dfrac{\partial \varepsilon_e}{\partial q}\right| + \left|\dfrac{\partial \varepsilon_{\ell at}}{\partial q}\right|} \qquad Q_\ell = -\frac{\dfrac{\partial W_e}{\partial q} + \dfrac{\partial W_\ell}{\partial q} + \dfrac{\partial G}{\partial q}}{\left|\dfrac{\partial \varepsilon_e}{\partial q}\right| + \left|\dfrac{\partial \varepsilon_\ell}{\partial q}\right|}$$

The usage of adapting grids allowed to perform all computations of grids with total number of nodes less than 100.

5 RESULTS

Regimes of irradiation with a Gaussian intensity distribution in the pulse $G(t) = G_0 exp\left(-(t/\tau)^2\right)$ were considered. Pulse duration τ_L = 10 ps. The maximum value of the intensity varied from G_0=3x10^9 to 5x10^{10} W/cm^2. Figures 2 and 3 show the time profiles of temperature and radiation at intensity G_0 = 3x10^9 W/cm^2. It can be seen that at such intensity the gap between the electron temperature and the temperature of the lattice is clearly seen, but the melting does not occur yet.

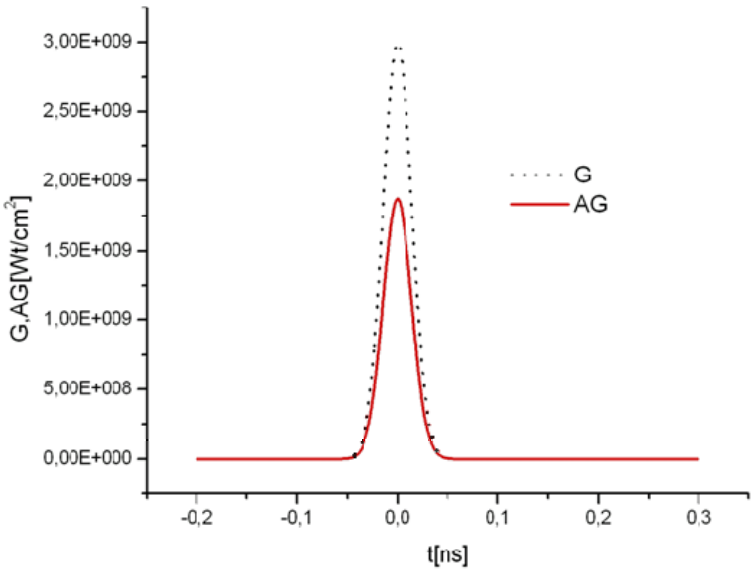

Figure 2. Time dependences of incident G (black dotted curve) and absorbed part AG (red solid curve) of laser radiation intensity, G_0=3x10^9 W/cm^2.

Increasing the intensity by one order of magnitude leads to the melting of silicon, which starts at the back front of the laser pulse. Typical time profiles of the laser radiation, surface temperatures, melting front velocity and (non)-equilibrium carrier concentrations on the surface for 3x10^{10} W/cm^2 energy pulse are shown in Fig. 4-7. Since the melting of lattice starts at the back front of the pulse, the maximum velocity υ_{sl} reaches relatively low value of ~ 27 m/s.

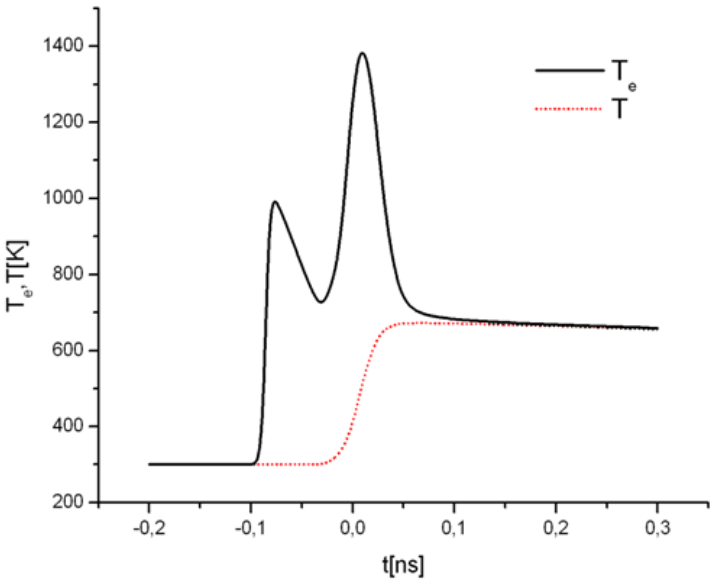

Figure 3. Time dependences of electron T_e (black solid curve) and lattice (red dotted curve) temperatures.

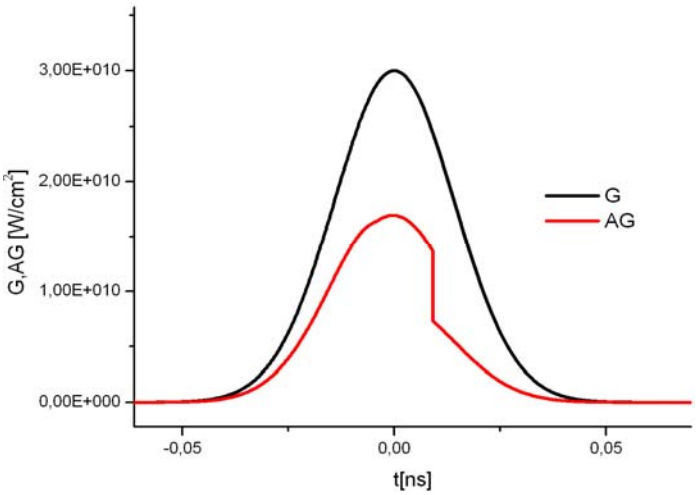

Figure 4. Time dependences of incident G (black curve) and absorbed part AG (red curve) of laser radiation intensity, $G_0=3x10^{10}$ W/cm^2.

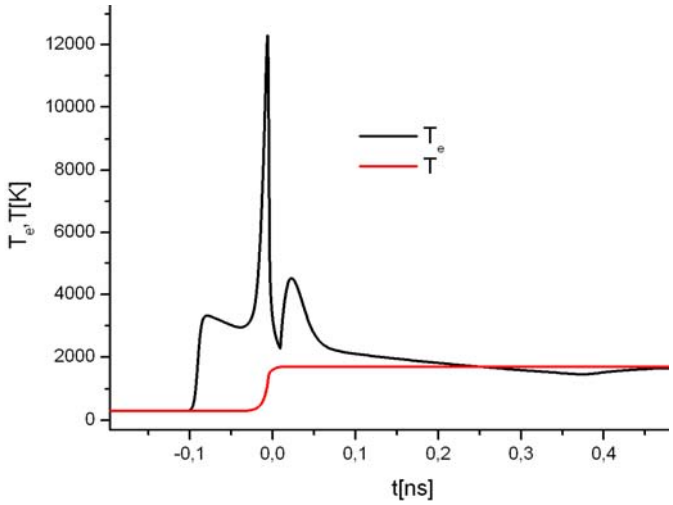

Figure 5. Time dependences of electron T_e (black curve) and lattice (red curve) temperatures.

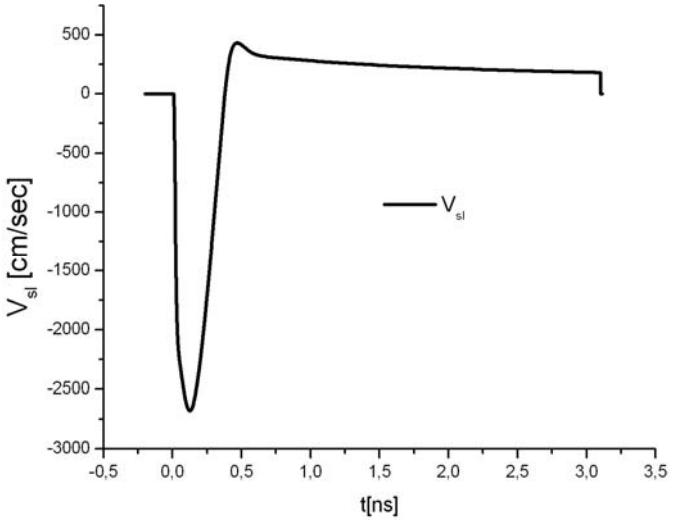

Figure 6. Time dependence of the melting velocity υ_{sl}.

As seen from the time dependences of temperatures (Fig.5 and Fig.9) throughout pulse duration there is a noticeable gap between the phonon and electron temperatures, which reaches 12000K at the peak of the pulse. By the end of the pulse the phonon and electron temperatures become equal.

Maximum melting front velocity reaches 27 m/s for $3x10^{10}$ W/cm^2 and 225 m/s for $5x10^{10}$ W/cm^2.

The presence of two peaks in the electron temperature in all regimes of irradiation should be noted, that indicates a change of the mechanism of absorption (photoprocesses replaced by inverse bremsstrahlung).

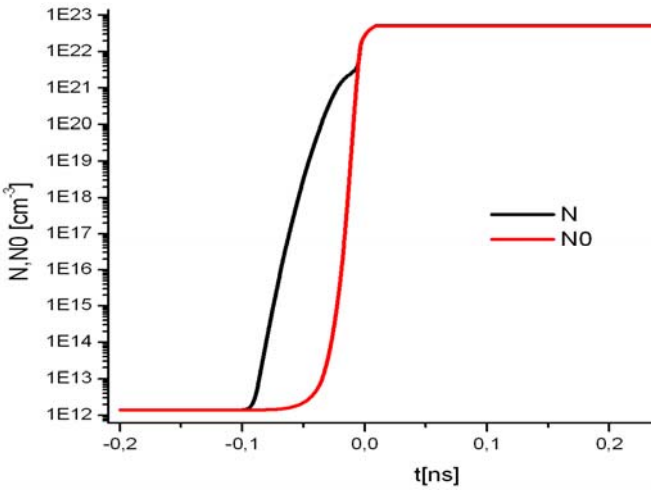

Figure 7. Time dependences of nonequilibrium N (black curve) and equilibrium N_0 (red curve) carrier concentrations on the surface.

A small change in the intensity of the radiation to $5x10^{10}$ W/cm^2 (Fig. 8-11) leads to the beginning of melting near the maximum of intensity that provides high value of melting velocity υ_{sl} =225 m/s and the gap between temperatures.

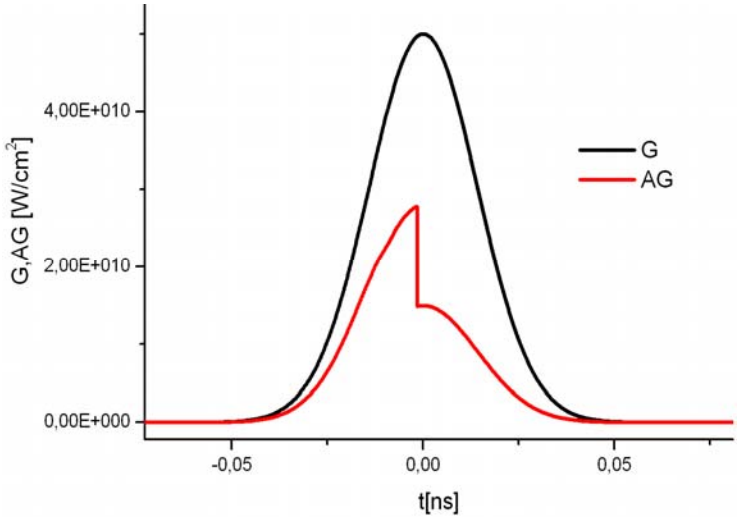

Figure 8. Time dependences of incident G (black curve) and absorbed part AG (red curve) of laser radiation intensity, G_0=$5x10^{10}$ W/cm^2.

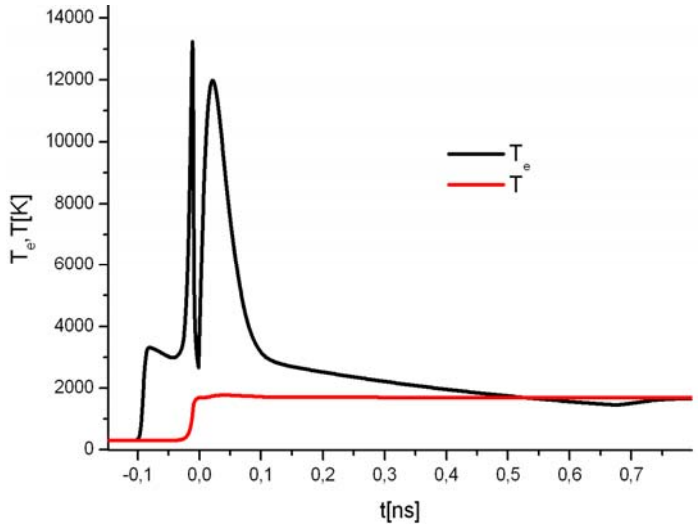

Figure 9. Time dependences of electron T_e (black curve) and lattice (red curve) temperatures.

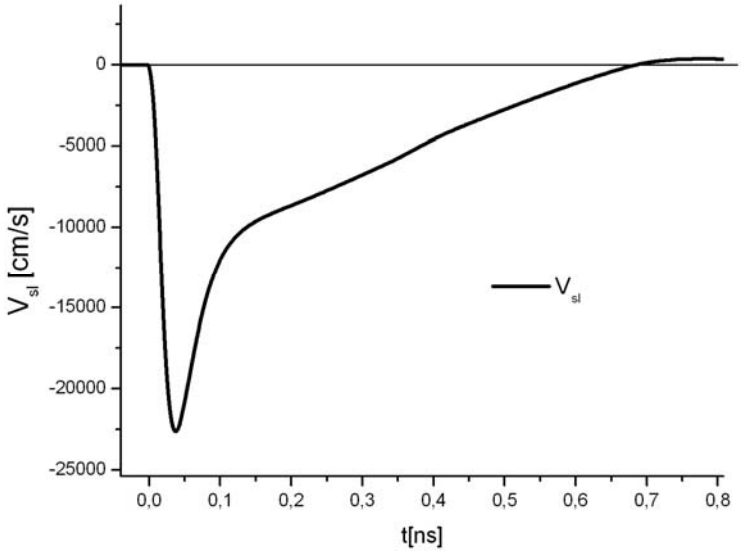

Figure 10. Time dependence of the melting velocity υ_{sl}.

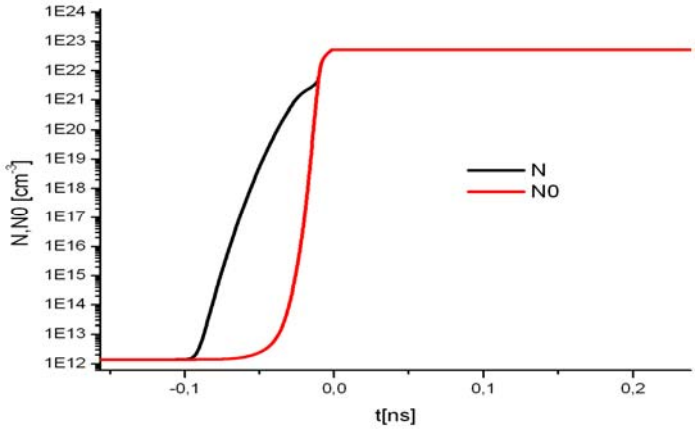

Figure 11. Time dependences of nonequilibrium N (black curve) and equilibrium N_0 (red curve) carrier concentrations on the surface.

4 CONCLUSION

Application of dynamic adaptation method to the numerical solution of the problems of non-equilibrium heating and phase transformations in semiconductor materials was considered. Computational features of these problems are the presence of two moving interphase boundaries and the presence of regions of rapid change of the solution components with different scales in space and time. The use of arbitrary time-dependent system of coordinates allows us to construct computational grids with a constant number of nodes in regions with moving boundaries and concentrate grid points in regions of large gradients of solutions.

Two functions of coordinate transformation by which we make controlled node distribution for nonlinear systems of differential equations of parabolic type were defined.

Numerical solution of two typical regimes of laser irradiation on the crystalline silicon was obtained.

Acknowledgment. This study was partly supported by RFBR grants 13-07-00597-a, 12-07-00436-a.

REFERENCES

[1] K.Sokolowski-Tinten, D. von der Linde (2000), "Generation of dense electron hole plasmas in silicon", *Phys. Rev. B*, 61, pp. 2643-2650.

[2] P.Allenspacher, B.Huttner, W.Riede (2003), "Ultrashort pulse damage of Si and Ge semiconductors", *SPIE*, 4932, 2003, pp. 358-365.

[3] V.I.Mazhukin, A.V.Mazhukin (2007), "Dynamic adaptation in parabolic equations", *Computational Mathematics and Mathematical Physics*, vol. 47, 11, pp. 1913-1936.

[4] V.I.Mazhukin, "Kinetics and Dynamics of Phase Transformations in Metals Under Action of Ultra-Short High-Power Laser Pulses", *Laser Pulses – Theory, Technology, and Applications* Ed. by I. Peshko, Chapter 8, 2012, pp-219-276.

[5] V.I.Mazhukin, M.M.Demin, A.V.Shapranov, I.Smurov. The method of construction dynamically adapting grids for problems of unstable laminar combustion. *Numerical Heat Transfer, Part B: Fundamentals,* 2003, vol.44, № 4, pp. 387 - 415.

[6] V.I.Mazhukin, I. Smurov, C. Dupuy, D. Jeandel. Simulation of Laser Induced Melting and Evaporation Processes in Superconducting. *J. Numerical Heat Transfer Part A*, 1994, v. 26, pp. 587-600.

[7] A.V.Mazhukin. Dynamic adaptation in convection — diffusion equations. *Computational methods in applied mathematics*, vol.8(2008), No.2, pp.171–186.

[8] V.I.Mazhukin, A.A.Samarskii, O.Kostelianos, A.V.Shapranov. Dynamic adaptation method for nonstationary problems with large gradients. *Mathematical modeling*, 1993, vol. 5, N 4, pp. 32-56.